Proceedings of the
44th IEEE Conference on Decision and Control, and
the European Control Conference 2005
Seville, Spain, December 12-15, 2005

Nonlinear Discrete-Time Control Approaches for Underactuated Manipulators

Dirk Weidemann, Norbert Scherm, Bodo Heimann, and Houssem Abdellatif

Abstract— **In this paper, we propose two nonlinear discrete-time control approaches for underactuated manipulators operating in the horizontal plane which are equipped with passive joints. The first control approach is based on an extended linearization. It can be applied to different kinds of underactuated systems such as a cart-pole system or a highly underactuated manipulator. A manipulator is called a highly underactuated manipulator if it has no braking mechanisms and more passive than active joints. However, the control approach mentioned above performs well only if the errors are sufficiently small. Therefore, a discrete-time feedback controller based on nonlinear online optimization is proposed also to counteract large trajectory deviations. In order to reduce the computation time, we present an initialization strategy of the nonlinear online optimization considering the relation between both controllers. Experimental results of both controller are reported to demonstrate advantages and drawbacks.**

I. INTRODUCTION

For more than a decade underactuated manipulators have been under investigation. In [1], one of the first results on these systems is presented. An underactuated system is characterized by having more generalized coordinates than actuators. Control of underactuated manipulators with passive joints operating in the horizontal plane is a special challenge. Since the dynamics of these manipulators are not affected by gravitational terms a linearization about an equilibrium point leads to a linear system which is not controllable. The loss of controllability is due to the fact that the dynamics are zero at an equilibrium point. Speaking in physical terms, the manipulator is only controllable if the dynamics are high enough. As a consequence the manipulators mentioned above can not be asymptotically stabilized at an equilibrium point by linear state feedback controllers. Moreover, the same stabilization task can not be done either using smooth nonlinear state feedback controllers, cf. [2].

As already noted, it is difficult or even not possible to control the manipulator if the dynamics are slow. However, typical motions sequences of these manipulators are rest to rest motions such that we have to deal with a time period at the end of the motion in which the dynamics are slow or almost zero. In order to reduce this time period as much as possible we adopt a discrete-time control approach. In contrast to the commonly used continuous-time control approach with an infinite settling time a discrete-time control approach offers the possibility to set up a controller with finite settling time, i.e. a dead-beat controller. Due to the finite settling time the time period in which the system is almost not controllable can be shortened significantly.

A discrete-time control approach for an underactuated manipulator is proposed in [3] for the first time. The same approach is also used for the swing up problem of a cart-pole system [4] and for a highly underactuated manipulator [5]. A manipulator is denoted as a highly underactuated manipulator if it is equipped with no braking mechanisms and has more passive than active joints. Both manipulators considered in [3] and [5] are operating in the horizontal plane. Even though we already reported some simulation results in [5] to our best knowledge this is the first time that experimental results of a highly underactuated manipulator are presented. In [6], another discrete-time control method is proposed for underactuated manipulators that can be transformed into a so called *chained form*. Nevertheless, the latter approach can be used only for a restricted class of manipulators.

The control approach proposed first, which is applied to a highly underactuated manipulator, is based on an extended linearization. This approach is efficient only for small errors. Therefore, also a feedback controller based on a nonlinear online optimization is proposed to overcome this drawback. The presented initialization strategy exploits the relation between the controller based on an extended linearization and the controller based on a nonlinear online optimization. Furthermore, the online optimization is done on shrinking horizons instead of a receding horizon to retain the relation between both controllers. Experimental results concerning a highly underactuated manipulator and a 2-DOF underactuated manipulator are presented to demonstrate advantages and drawbacks of both controllers. For the first system a controller based on an extended linearization is applied, whereas the second system is controlled using the approach based on a nonlinear optimization.

The paper is structured as follows. The dynamics of the underactuated manipulators and the discrete-time notation are given in section II and section III, respectively. In section IV and V the feedback controller based on an extended linearization and on an online optimization are presented. Finally the experimental results are given in section VI.

This work was supported by the DFG (Deutsche Forschungsgemeinschaft) in Germany under Grant HE2445/2-1

D. Weidemann, B. Heimann, and H. Abdellatif are with the Center of Mechatronics, University of Hannover, Appelstraße 11, D-30167 Hannover, Germany {weidemann, heimann, abdellatif}@mzh.uni-hannover.de

N. Scherm is with the Institute of Automatic Control, University of Hannover, Appelstraße 11, D-30167 Hannover, Germany. *Current Address*: Rheinmetall Defence Electronics, Brüggeweg 54, D-28309 Bremen, Germany. scherm.n@rheinmetall-de.com

0-7803-9568-9/05/$20.00 ©2005 IEEE

II. MODEL OF MANIPULATOR

The manipulators considered in this paper are shown in Fig. 1. All joints are rotational joints without limits, but in both cases only the first joint is equipped with an actuator. In addition, the manipulators operate in the horizontal plane such that the dynamic equations do not contain gravitational terms. The dynamic equations for both manipulators are

$$\boldsymbol{M}(\boldsymbol{q}(t))\ddot{\boldsymbol{q}}(t) + \boldsymbol{c}(\boldsymbol{q}(t), \dot{\boldsymbol{q}}(t)) + \boldsymbol{d}(\dot{\boldsymbol{q}}(t)) = \begin{bmatrix} \tau(t) \\ \mathbf{0} \in \mathbb{R}^{\{1,2\}} \end{bmatrix},$$

where $\boldsymbol{q}(t) \in \mathbb{R}^n$ with $n \in \{2, 3\}$ is the vector of generalized coordinates and $\boldsymbol{M}(\cdot)$ is the symmetric mass matrix. Furthermore, $\boldsymbol{c}(\cdot,\cdot)$ is the vector of centrifugal and Coriolis torques, $\boldsymbol{d}(\cdot,\cdot)$ is the sum of viscous damping and dry friction torques (cf. [5] for a detailed description of $\boldsymbol{d}(\cdot,\cdot)$), and $\tau(t)$ is the torque applied to the active joint.

Let the state vector of the underactuated manipulators be defined by $\boldsymbol{x}(t) = [\boldsymbol{x}_1^T(t), \boldsymbol{x}_2^T(t)]^T = [\boldsymbol{q}^T(t), \dot{\boldsymbol{q}}^T(t)]^T$ such that the state space representation of the manipulator is

$$\begin{aligned} \dot{\boldsymbol{x}}_1(t) &= \boldsymbol{x}_2(t), \\ \dot{\boldsymbol{x}}_2(t) &= -\boldsymbol{M}^{-1}(\boldsymbol{x}_1(t))\left[\boldsymbol{c}(\boldsymbol{x}_1(t), \boldsymbol{x}_2(t)) + \boldsymbol{d}(\boldsymbol{x}_2(t))\right] + \\ &\quad \boldsymbol{M}^{-1}(\boldsymbol{x}_1(t)) \begin{bmatrix} u(t) \\ \mathbf{0} \in \mathbb{R}^{\{1,2\}} \end{bmatrix} \end{aligned}$$

with $u(t) = \tau(t)$. If a controller is applied for the acceleration of the active joint $\ddot{q}_1(t)$ then the input variable is $u(t) = \ddot{q}_1(t)$ instead of $u(t) = \tau(t)$.

In general, the continuous-time nonlinear state space representation is given by the vector notation

$$\dot{\boldsymbol{x}}(t) = \boldsymbol{f}_{\mathrm{c}}(\boldsymbol{x}(t), u(t)), \tag{1}$$

where $\boldsymbol{f}_{\mathrm{c}}(\cdot,\cdot) : \mathbb{R}^{2n} \times \mathbb{R} \mapsto \mathbb{R}^{2n}$ is a real valued continuously differentiable function.

III. DISCRETE-TIME REPRESENTATION

Since the presented approach is based on a digital controller, both measurements and control actions are done at discrete-time instants $t \in \{0, T, 2T, \dots\}$, where $T > 0$ denotes the sampling time. If a zero-order hold element is applied the input $u(t)$ is constant on intervals of equal length T, i.e. $u(t) = u_k$ on intervals $t \in [kT, (k+1)T)$. Let the discrete-time system

$$\boldsymbol{x}_{k+1} = \boldsymbol{f}(\boldsymbol{x}_k, u_k) \tag{2}$$

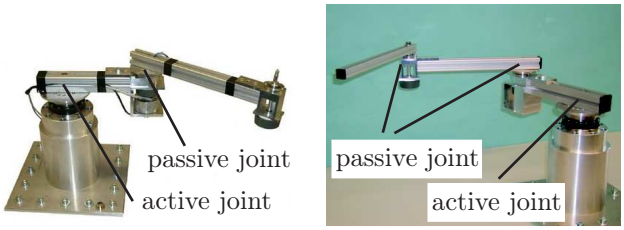

(a) Underactuated manipulator (one passive joint)

(b) Highly underactuated manipulator (two passive joints)

Fig. 1. Underactuated manipulators operating in the horizontal plane

be the corresponding representation of the continuous-time system given by (1). The computation of 2 is described in detail in [3]. Performing a left-shift of (2) and substituting $\boldsymbol{x}_{k+1}$ by $\boldsymbol{f}(\boldsymbol{x}_k, u_k)$ leads to the recursive representation $\boldsymbol{x}_{k+2} = \boldsymbol{f}(\boldsymbol{f}(\boldsymbol{x}_k, u_k), u_{k+1}) = \boldsymbol{f}^{[2]}(\boldsymbol{x}_k, \boldsymbol{u}_k)$ with $\boldsymbol{u}_k = [u_k, u_{k+1}]^T$. In general, the state $\boldsymbol{x}_{k+m}$ is given by

$$\boldsymbol{x}_{k+m} = \boldsymbol{f}^{[m]}(\boldsymbol{x}_k, \boldsymbol{u}_k) \tag{3}$$

with $\boldsymbol{f}^{[m]}(\cdot,\cdot) : \mathbb{R}^{2n} \times \mathbb{R}^m \mapsto \mathbb{R}^{2n}$ and the input vector $\boldsymbol{u}_k = [u_k, u_{k+1}, \dots, u_{k+m-1}]^T$.

IV. FEEDBACK CONTROL BY EXTENDED LINEARIZATION

Consider the system given by (3). Without loss of generality we set $k = 0$ in this section. Suppose an input sequence $\boldsymbol{u}_0$ is computed such that the system given by $\boldsymbol{x}_m = \boldsymbol{f}^{[m]}(\boldsymbol{x}_0, \boldsymbol{u}_0)$ is steered from a desired starting position to a desired final position. Here and throughout this paper a hat $\hat{(\cdot)}$ indicates the ideal motion. Consequently $\hat{\boldsymbol{x}}_0$, $\hat{\boldsymbol{x}}_m$, and $\hat{\boldsymbol{u}}_0 = [\hat{u}_0, \hat{u}_1, \dots, \hat{u}_{m-1}]^T$ denote the desired starting position, the desired final position, and the input sequence of the ideal motion, respectively. An appropriate path planning method to compute $\hat{\boldsymbol{u}}_0$ is given in [5].

Ideally, if the system is not disturbed, the feedforward control input sequence $\hat{\boldsymbol{u}}_0$ is sufficient to steer the system along the desired trajectory given by $\hat{\boldsymbol{x}}_k$, $k \in \{0, 1, \dots, m\}$. In practice the system is subject to perturbations such that a feedback controller

$$\boldsymbol{u}_0 = \boldsymbol{r}_{[m]}(\boldsymbol{x}_0) \tag{4}$$

with $\boldsymbol{r}_{[m]}(\cdot) : \mathbb{R}^{2n} \mapsto \mathbb{R}^m$ is necessary to stabilize the desired motion. The feedback controller provides the feedforward control input sequence $\boldsymbol{r}_{[m]}(\hat{\boldsymbol{x}}_0) = \hat{\boldsymbol{u}}_0 = [\hat{u}_0, \hat{u}_1, \dots, \hat{u}_{m-1}]^T$ if no initial errors exist, i.e. $\boldsymbol{x}_0 = \hat{\boldsymbol{x}}_0$. The control formula $\boldsymbol{r}_{[m]}(\boldsymbol{x}_0)$ can be derived by an extended linearization as presented in the following.

Assume the initial errors are sufficiently small $||\boldsymbol{x}_0 - \hat{\boldsymbol{x}}_0|| \approx 0$. Then feasible approximations of $\boldsymbol{r}(\boldsymbol{x}_0)$ and the state error $\boldsymbol{e}_m = \boldsymbol{x}_m - \hat{\boldsymbol{x}}_m = \boldsymbol{f}^{[m]}(\boldsymbol{x}_0, \boldsymbol{u}_0) - \hat{\boldsymbol{x}}_m$ are given by

$$\boldsymbol{r}(\boldsymbol{x}_0) = \boldsymbol{r}(\hat{\boldsymbol{x}}_0) + \boldsymbol{R}(\hat{\boldsymbol{x}}_0, \hat{\boldsymbol{u}}_0)[\boldsymbol{x}_0 - \hat{\boldsymbol{x}}_0] \tag{5}$$

and

$$\boldsymbol{e}_m = \underbrace{\left[\boldsymbol{A}(\hat{\boldsymbol{x}}_0, \hat{\boldsymbol{u}}_0) + \boldsymbol{S}(\hat{\boldsymbol{x}}_0, \hat{\boldsymbol{u}}_0)\boldsymbol{R}(\hat{\boldsymbol{x}}_0, \hat{\boldsymbol{u}}_0)\right]}_{=\boldsymbol{G}(\hat{\boldsymbol{x}}_0, \hat{\boldsymbol{u}}_0)} \boldsymbol{e}_0 \tag{6}$$

with the Jacobians $\boldsymbol{A}(\cdot,\cdot) = \frac{\partial}{\partial \hat{\boldsymbol{x}}_0}\boldsymbol{f}^{[m]}(\hat{\boldsymbol{x}}_0, \hat{\boldsymbol{u}}_0)$, $\boldsymbol{S}(\cdot,\cdot) = \frac{\partial}{\partial \hat{\boldsymbol{u}}_0}\boldsymbol{f}^{[m]}(\hat{\boldsymbol{x}}_0, \hat{\boldsymbol{u}}_0)$, and $\boldsymbol{R}(\cdot,\cdot) = \frac{\partial}{\partial \hat{\boldsymbol{x}}_0}\boldsymbol{r}(\hat{\boldsymbol{x}}_0)$. Both (5) and (6) represent a truncated Taylor series expansion of $\boldsymbol{r}(\boldsymbol{x}_0)$ and $\boldsymbol{e}_m = \boldsymbol{x}_m - \hat{\boldsymbol{x}}_m$ about $\hat{\boldsymbol{x}}_0$. As indicated by the arguments $\hat{\boldsymbol{x}}_0, \hat{\boldsymbol{u}}_0$ of the controller matrix $\boldsymbol{R}(\cdot,\cdot)$ an individual controller is necessary for each motion. Furthermore, the matrix $\boldsymbol{G}(\cdot,\cdot)$, which can be chosen arbitrarily, determines the error dynamics, e.g. a dead-beat controller can be derived by setting $\boldsymbol{G}(\cdot,\cdot) = \mathbf{0}$.

If $\boldsymbol{S}(\cdot,\cdot)$ has full row rank, solving the underdetermined problem

$$\min_{\boldsymbol{R}(\hat{\boldsymbol{x}}_0,\hat{\boldsymbol{u}}_0)\boldsymbol{e}_0} \left(m_{\mathrm{EL}}(\boldsymbol{R}(\hat{\boldsymbol{x}}_0,\hat{\boldsymbol{u}}_0)\boldsymbol{e}_0)\right) \tag{7}$$

with

$$m_{\mathrm{EL}}(\boldsymbol{R}(\hat{\boldsymbol{x}}_0,\hat{\boldsymbol{u}}_0)\boldsymbol{e}_0) = ||\boldsymbol{e}_m - \boldsymbol{G}(\hat{\boldsymbol{x}}_0,\hat{\boldsymbol{u}}_0)\boldsymbol{e}_0||^2 \tag{8}$$

in sense of a minimum norm approach yields the controller matrix

$$\boldsymbol{R}(\hat{\boldsymbol{x}}_0,\hat{\boldsymbol{u}}_0) = \boldsymbol{S}^{\dagger}(\hat{\boldsymbol{x}}_0,\hat{\boldsymbol{u}}_0)\left[\boldsymbol{G}(\hat{\boldsymbol{x}}_0,\hat{\boldsymbol{u}}_0) - \boldsymbol{A}(\hat{\boldsymbol{x}}_0,\hat{\boldsymbol{u}}_0)\right] \tag{9}$$

where $\boldsymbol{S}^{\dagger}(\cdot,\cdot) = \boldsymbol{S}^T(\cdot,\cdot)[\boldsymbol{S}(\cdot,\cdot)\boldsymbol{S}^T(\cdot,\cdot)]^{-1}$ denotes the right pseudoinverse. Since the matrix $\boldsymbol{S}(\cdot,\cdot)$ is often ill conditioned or even singular we use the regularized minimization problem

$$\min_{\boldsymbol{R}(\hat{\boldsymbol{x}}_0,\hat{\boldsymbol{u}}_0)\boldsymbol{e}_0} \left(m_{\mathrm{EL}}(\boldsymbol{R}(\hat{\boldsymbol{x}}_0,\hat{\boldsymbol{u}}_0)\boldsymbol{e}_0) + \mu_{\mathrm{EL}}^2\,||\boldsymbol{R}(\hat{\boldsymbol{x}}_0,\hat{\boldsymbol{u}}_0)\boldsymbol{e}_0||^2\right) \tag{10}$$

instead of (7) to derive the controller matrix. The latter approach, which is an overdetermined least squares problem due to the regularization, improves both the reliability (i.e. limited amplitude) of $\boldsymbol{R}(\cdot,\cdot)\boldsymbol{e}_0$ and the behavior of the closed loop. In (10) $\mu_{\mathrm{EL}} > 0$ characterizes the *Tikhonov* regularization parameter. The solution to (10) is given by (9) if the regularized right pseudoinverse $\boldsymbol{S}^{\dagger}_{\mu_{\mathrm{EL}}}(\cdot,\cdot) = \boldsymbol{S}^T(\cdot,\cdot)[\boldsymbol{S}(\cdot,\cdot)\boldsymbol{S}^T(\cdot,\cdot) + \mu_{\mathrm{EL}}^2\boldsymbol{I}]^{-1}$ is substituted for $\boldsymbol{S}^{\dagger}(\cdot,\cdot)$ in (9). Note that left and right regularized pseudoinverse are identical as long as no scaling is adopted in (10).

The working scheme of the controller given by (4) is shown in Fig. 2 where the input sequences of the feedforward controller $\hat{\boldsymbol{u}}_0$ and the feedback controller $\boldsymbol{u}_0$ are depicted by a solid and a dashed line, respectively. Furthermore, the circle and the black bar indicate the measurement time instant and the time period in which the controller is valid.

A. Tracking Controller

The controller given by (4) counteracts only initial errors because only one measurement is done at the beginning of the motion. Besides initial errors, further perturbations such as measuring errors and mismatches between the mathematical model and the real system have to be taken into account. In order to respond to state errors that arise during the time interval $t \in [\,0, mT]$, we utilize several controllers with shorter time periods. For each of these shorter time periods of equal length $t \in [\,kT_{\mathrm{S}}, (k+m_{\mathrm{S}})T_{\mathrm{S}})$ with $T_{\mathrm{S}} = \frac{T}{a\,m_{\mathrm{S}}}$, $k \in \{0, m_{\mathrm{S}}, 2m_{\mathrm{S}}, \ldots, (am-1)m_{\mathrm{S}}\}$, and $a \in \mathbb{N}$ an individual controller $\boldsymbol{r}_{[m_{\mathrm{S}}]}(\boldsymbol{x}_k)$ is computed, which leads to a tracking controller. This approach is illustrated in Fig. 3 with $a = 1$ and $m_{\mathrm{S}} = 8$. In Fig. 3 both the circles and the bar display the same as in Fig. 2.

V. FEEDBACK CONTROL BY NONLINEAR ONLINE OPTIMIZATION

In the following we focus on computing a controller for one subinterval $t \in [kT_{\mathrm{S}}, (k+m_{\mathrm{S}})T_{\mathrm{S}})$. Even though the feedback controller based on an extended linearization performs well for several kinds of underactuated systems a significant drawback of this controller is that the state errors have to be sufficiently small. A more general approach to derive a feedback controller is to solve the nonlinear least squares problem

$$\min_{\boldsymbol{r}_{[m_{\mathrm{S}}]}(\boldsymbol{x}_k)} \left|\left|\boldsymbol{e}_{k+m_{\mathrm{S}}}(\boldsymbol{x}_k, \boldsymbol{r}_{[m_{\mathrm{S}}]}(\boldsymbol{x}_k))\right|\right|^2 \tag{11}$$

with $\boldsymbol{e}_{k+m_{\mathrm{S}}}(\cdot,\cdot) = \boldsymbol{f}^{[m_{\mathrm{S}}]}(\boldsymbol{x}_k, \boldsymbol{r}_{[m_{\mathrm{S}}]}(\boldsymbol{x}_k)) - \hat{\boldsymbol{x}}_{k+m_{\mathrm{S}}}$ by a nonlinear optimization method. The problem given by (11) can be solved iteratively. Performing a linearization of (11) about the current iterate $\boldsymbol{r}^i_{[m_{\mathrm{S}}]}(\boldsymbol{x}_k)$ results in

$$\min_{\boldsymbol{r}_{[m_{\mathrm{S}}]}(\boldsymbol{x}_k)} \left(m^i_{\mathrm{NO}}(\boldsymbol{r}_{[m_{\mathrm{S}}]}(\boldsymbol{x}_k))\right) \tag{12}$$

where

$$m^i_{\mathrm{NO}}(\boldsymbol{r}_{[m_{\mathrm{S}}]}(\boldsymbol{x}_k)) = \Big|\Big|\boldsymbol{e}^i_{k+m_{\mathrm{S}}}(\boldsymbol{x}_k, \boldsymbol{r}^i_{[m_{\mathrm{S}}]}(\boldsymbol{x}_k)) + \boldsymbol{S}(\boldsymbol{x}_k, \boldsymbol{r}^i_{[m_{\mathrm{S}}]}(\boldsymbol{x}_k))\left[\boldsymbol{r}_{[m_{\mathrm{S}}]}(\boldsymbol{x}_k) - \boldsymbol{r}^i_{[m_{\mathrm{S}}]}(\boldsymbol{x}_k)\right]\Big|\Big|^2 \tag{13}$$

characterizes the quadratic model and $\boldsymbol{e}^i_{k+m_{\mathrm{S}}}(\cdot,\cdot) = \boldsymbol{f}^{[m_{\mathrm{S}}]}(\boldsymbol{x}_k, \boldsymbol{r}_{[m_{\mathrm{S}}]}(\boldsymbol{x}_k)) - \hat{\boldsymbol{x}}_{k+m_{\mathrm{S}}}$ the current state error. However, as in the case of the controller based on an extended linearization (cf. section IV) the Jacobian $\boldsymbol{S}(\cdot,\cdot) = \frac{\partial}{\partial \boldsymbol{r}^i_{[m_{\mathrm{S}}]}(\boldsymbol{x}_k)} \boldsymbol{f}^{[m_{\mathrm{S}}]}(\boldsymbol{x}_k, \boldsymbol{r}^i_{[m_{\mathrm{S}}]}(\boldsymbol{x}_k))$ is ill conditioned. Therefore,

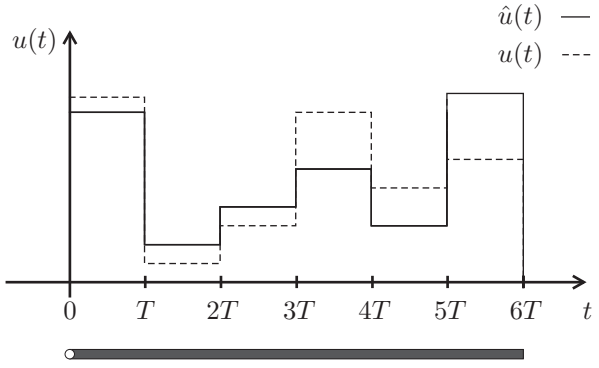

Fig. 2. Working scheme of initial error controller $\boldsymbol{r}(\boldsymbol{x}_0)$

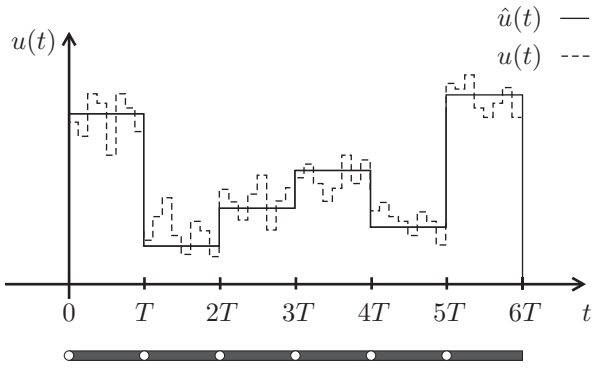

Fig. 3. Working scheme of tracking controller $\boldsymbol{r}_{[m_{\mathrm{S}}]}(\boldsymbol{x}_k)$, $k \in \{0, m_{\mathrm{S}}, 2m_{\mathrm{S}}, \ldots, 5m_{\mathrm{S}}\}$

it is necessary to stabilize the minimization problem (12) by some kind of regularization to avoid divergence of the iteration process due to large step sizes, cf. [7]. If a *Tikhonov* regularization [7] is applied, instead of (12) the problem

$$\min_{\boldsymbol{r}_{[m_\mathrm{S}]}(\boldsymbol{x}_k)} \left(m^i_{\mathrm{NO}}(\boldsymbol{r}_{[m_\mathrm{S}]}(\boldsymbol{x}_k)) + \mu^2_{\mathrm{NO}} \left|\left| \boldsymbol{r}_{[m_\mathrm{S}]}(\boldsymbol{x}_k) \right|\right|^2 \right) \quad (14)$$

has to be solved in each iteration step. The latter approach is known as *Levenberg-Marquardt* method (cf. [8]) and the weighting factor $\mu_{\mathrm{NO}} > 0$ in (14) denotes the *Levenberg-Marquardt* parameter. Solving (14) yields the next iterate

$$\boldsymbol{r}^{i+1}_{[m_\mathrm{s}]}(\boldsymbol{x}_k) = \boldsymbol{r}^{i}_{[m_\mathrm{s}]}(\boldsymbol{x}_k) - \boldsymbol{S}^{\dagger}_{\mu_{\mathrm{NO}}}(\boldsymbol{x}_k, \boldsymbol{r}^{i}_{[m_\mathrm{s}]}(\boldsymbol{x}_k)) \left[\boldsymbol{e}^{i}_{k+m_\mathrm{S}}(\boldsymbol{x}_k, \boldsymbol{r}^{i}_{[m_\mathrm{S}]}(\boldsymbol{x}_k)) \right] \quad (15)$$

with the regularized pseudoinverse $\boldsymbol{S}^{\dagger}_{\mu_{\mathrm{NO}}}(\cdot,\cdot) = \boldsymbol{S}^T(\cdot,\cdot) \times [\boldsymbol{S}(\cdot,\cdot)\boldsymbol{S}^T(\cdot,\cdot) + \mu^2_{\mathrm{NO}}\boldsymbol{I}]^{-1}$. Provided that the minimization process converges the solution to (11) is indicated by $\hat{\boldsymbol{r}}_{[m_\mathrm{S}]}(\boldsymbol{x}_k) = [\hat{r}_k(\boldsymbol{x}_k), \hat{r}_{k+1}(\boldsymbol{x}_k), \ldots, \hat{r}_{k+m_\mathrm{S}-1}(\boldsymbol{x}_k)]^T$.

A. Generation of Initial Values

Although it is possible to counteract large errors using a nonlinear optimization, the major problem computing such a feedback controller is that (11) has to be solved online. The aim is to provide a good initial value $\boldsymbol{r}^0_{[m_\mathrm{S}]}(\boldsymbol{x}_k)$ such that the calculation time can be reduced as much as possible. Furthermore, feedback delays have to be avoided, see section V-B.

In order to derive an initial value $\boldsymbol{r}^0_{[m_\mathrm{S}]}(\boldsymbol{x}_k)$ we take advantage of the relation between the feedback controller given by (11) and the feedback controller based on an extended linearization, cf. (9).

In case the system is close to the desired trajectory $||\boldsymbol{x}_k - \hat{\boldsymbol{x}}_k|| \approx 0$ the nonlinear controller $\boldsymbol{r}_{[m_\mathrm{S}]}(\boldsymbol{x}_k)$ can be substituted by the truncated Taylor series expansion (5) if we replace 0, m by k, m_S. Therefore, a linearization of (11) about $\hat{\boldsymbol{x}}_k$ yields

$$\min_{\boldsymbol{R}(\hat{\boldsymbol{x}}_k,\hat{\boldsymbol{u}}_k)\boldsymbol{e}_k} (m_{\mathrm{NO,L}}(\boldsymbol{R}(\hat{\boldsymbol{x}}_k,\hat{\boldsymbol{u}}_k)\boldsymbol{e}_k)) \quad (16)$$

with

$$m_{\mathrm{NO,L}}(\boldsymbol{R}(\hat{\boldsymbol{x}}_k,\hat{\boldsymbol{u}}_k)\boldsymbol{e}_k) = ||(\boldsymbol{A}(\hat{\boldsymbol{x}}_k,\hat{\boldsymbol{u}}_k) + \boldsymbol{S}(\hat{\boldsymbol{x}}_k,\hat{\boldsymbol{u}}_k)\boldsymbol{R}(\hat{\boldsymbol{x}}_k,\hat{\boldsymbol{u}}_k))\,\boldsymbol{e}_k||^2 . \quad (17)$$

Comparing the solution to (16)

$$\boldsymbol{R}(\hat{\boldsymbol{x}}_k,\hat{\boldsymbol{u}}_k) = -\boldsymbol{S}^{\dagger}(\hat{\boldsymbol{x}}_k,\hat{\boldsymbol{u}}_k)\boldsymbol{A}(\hat{\boldsymbol{x}}_k,\hat{\boldsymbol{u}}_k) \quad (18)$$

with the controller matrix given by an extended linearization in (9) shows that both are the same if the controller based on an extended linearization is computed using a dead-beat approach. This relation between both controller is still valid if the minimization problem given by (16) is stabilized by a *Tikhonov* regularization using the parameter μ_{EL}. Therefore, the controller derived by an extended linearization is a special case of the controller based on online optimization if the errors are small.

Due to the relation between both controllers, the controller sequence

$$\boldsymbol{r}^0_{[m_\mathrm{S}]}(\boldsymbol{x}_k) = \hat{\boldsymbol{u}}_k + \boldsymbol{R}(\hat{\boldsymbol{x}}_k,\hat{\boldsymbol{u}}_k)[\boldsymbol{x}_k - \hat{\boldsymbol{x}}_k] \quad (19)$$

is used as initial value of the online optimization. The input sequence $\hat{\boldsymbol{u}}_k$ and the controller matrix $\boldsymbol{R}(\cdot,\cdot)$ can be calculated offline. A similar initialization technique for shrinking horizon problems is proposed in [9], [10] .

B. Avoidance of Feedback Delays

Despite the fact that the initialization technique proposed by (19) is used, frequently several iterations are required to minimize (11). This holds true especially for a system which is subject to large errors. Thus, it is not possible to apply the input sequence immediately to the system at the sampling time instant $t = kT_\mathrm{S}$ which results in a significant feedback delay. In order to avoid feedback delays we measure $\boldsymbol{x}_{k-1}$ and use a prediction $\tilde{\boldsymbol{x}}_k = \boldsymbol{f}(\boldsymbol{x}_{k-1}, u_{k-1})$ to start the minimization process. As a result, the minimization process is performed during the sampling interval $t \in [(k-1)T_\mathrm{S}, kT_\mathrm{S})$.

C. Online Optimization on Shrinking Horizons

In the following a prediction at an arbitrary time instant is indicated by $\tilde{\boldsymbol{x}}_{k+j} = \boldsymbol{f}(\boldsymbol{x}_{k+j-1}, u_{k+j-1})$. Assume p iterations being performed during the time interval $t \in [(k-1)T_\mathrm{S}, kT_\mathrm{S})$. The input sequence $\boldsymbol{r}^p_{[m_\mathrm{S}]}(\tilde{\boldsymbol{x}}_k)$ that has been calculated after p iterations is used whether $\boldsymbol{r}^p_{[m_\mathrm{S}]}(\tilde{\boldsymbol{x}}_k)$ is a solution or only a suboptimal solution to the optimization problem given by (11). A similar approach with only one iteration is presented in [11]. As it is common in model predictive control (cf. [9], [10], [11]) only the first element of $\boldsymbol{r}^p_{[m_\mathrm{S}]}(\tilde{\boldsymbol{x}}_k)$ is applied to the system. In most cases of model predictive control a moving horizon approach is adopted, which is also called a receding horizon approach.

In contrast to a moving horizon approach, which usually applies a constant horizon with a constant dimension of optimization variables, we use a fixed final time and reduce successively the dimension of optimization variables to compute the next control input. This approach leads consequently to a reduced horizon and is called a shrinking horizon approach, cf. [9], [10]. A modification of (11) that also includes the reduced optimization problem is given by

$$\min_{\boldsymbol{r}_{[m_\mathrm{S}-j]}(\tilde{\boldsymbol{x}}_{k+j})} \left|\left| \boldsymbol{e}_{k+m_\mathrm{S}}(\tilde{\boldsymbol{x}}_{k+j}, \boldsymbol{r}_{[m_\mathrm{S}-j]}(\tilde{\boldsymbol{x}}_{k+j})) \right|\right|^2 \quad (20)$$

with $\boldsymbol{e}_{k+m_\mathrm{S}}(\cdot,\cdot) = \boldsymbol{f}^{[m_\mathrm{S}-j]}(\tilde{\boldsymbol{x}}_{k+j}, \boldsymbol{r}_{[m_\mathrm{S}-j]}(\tilde{\boldsymbol{x}}_{k+j})) - \hat{\boldsymbol{x}}_{k+m_\mathrm{S}}$ and $\boldsymbol{r}_{[m_\mathrm{S}-j]}(\cdot) : \mathbb{R}^{2n} \mapsto \mathbb{R}^{m_\mathrm{S}-j}$, $j \in \{0, 1, \ldots, m_\mathrm{S}-1\}$. If $j \neq 0$ then the initialization of the reduced minimization problem is done by all elements but the first of the previous suboptimal solution $\boldsymbol{r}^0_{[m_\mathrm{S}-j]}(\tilde{\boldsymbol{x}}_{k+j}) = [r^p_{k+j}(\tilde{\boldsymbol{x}}_{k+j-1}), \ldots, r^p_{k+m_\mathrm{S}-1}(\tilde{\boldsymbol{x}}_{k+j-1})]^T$.

Even though it is possible to enlarge the region of convergence using this shrinking horizon approach (cf. section VI-B) a drawback is still the limited computation time[1]. Due

[1]The manipulator is controlled by a VME-BUS computer with a 366 MHz PowerPC CPU and 64MB RAM running the real time operating system RTOS-UH (**R**eal **T**ime **O**perating **S**ystem-**U**niversity **H**annover).

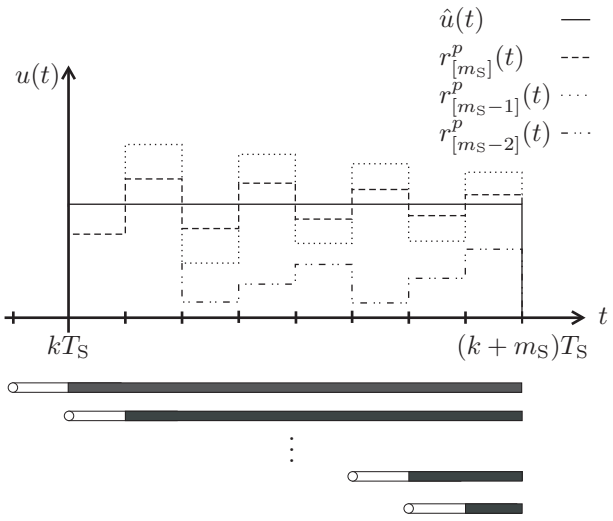

Fig. 4. Working scheme using shrinking horizon

to this restriction we are not able to use this controller in connection with the highly underactuated manipulator.

An illustration of the working scheme applying a shrinking horizon is shown for one arbitrary subinterval in Fig. 4 with $m_S = 8$ and $a = 1$. The circles represent the sampling time instant. Furthermore, the white bars display the time period in which both prediction and optimization are done. The horizon length of the corresponding optimization problem is shown by a black bar. As in Fig. 2 and Fig. 3 the solid line depicts the feedforward control input. The dashed line shows the feedback input sequence that is result of the first optimization stage using the full horizon length $t \in [kT_S, (k+m_S)T_S)$. As mentioned above only the first element of the input sequence is applied to the system. Reducing the horizon length leads to the second optimization stage which considers the horizon $t \in [(k+1)T_S, (k+m_S)T_S)$. The resulting input sequence is given by a dotted line. In addition, the result of the third optimization stage with the horizon length $t \in [(k+2)T_S, (k+m_S)T_S)$ is depicted by a dashed-double-dotted line. Note that the shrinking horizon approach has to be done not only once but once for each time period $t \in [kT_S, (k+m_S)T_S)$ with $k \in \{0, m_S, 2m_S, \ldots, (am-1)m_S\}$.

VI. EXPERIMENTAL RESULTS

In the following we present one motion of each manipulator shown in Fig. 1 to demonstrate advantages and drawbacks of both controllers. Both motions are rest to rest motions such that the desired velocities at the start and final position are zero. In all figures the desired trajectories $\hat{q}_{\{2,3\}}(\hat{q}_1)$ are given by solid lines, feedforward trajectories $q_{\{2,3\}}(q_1)_{\mathrm{FF}}$ by dash-dotted lines, and trajectories $q_{\{2,3\}}(q_1)_{\mathrm{EL}}$ using a controller based on an extended linearization by dotted lines. Since in Fig. 6(b) no feedforward control results are presented the trajectory $q_2(q_1)_{\mathrm{NO}}$ using a controller based on a nonlinear online optimization is shown also by dash-dotted lines. In order to keep the figures simple only the sampling instants kT with $k \in \{0, 2m_S, 4m_S, \ldots, 12m_S\}$ are depicted. The sampling instants are indicated by $\bigcirc$ for the desired trajectory, by $\Diamond$ for the feedforward trajectory, by $\triangledown$ for the feedback trajectory using an extended linearization and by $\square$ for the feedback trajectory using the online optimization in Fig. 6(b). Furthermore, we apply the sample times $T = 0.384$[s], $T_S = \frac{T}{a} = 0.192$[s] with $a = 2$ and the error dynamics $\boldsymbol{G}(\hat{\boldsymbol{x}}_k, \hat{\boldsymbol{u}}_k) = \boldsymbol{0}$ for both motions.

A. Extended Linearization

The first motion is a 90° turn of the highly underactuated manipulator depicted in Fig. 1(b) from $q_1(0) = 0°$, $q_2(0) = 0°$, $q_3(0) = 0°$ to $q_1(mT) = 90°$, $q_2(mT) = 0°$, $q_3(mT) = 0°$. The corresponding controller based on an extended linearization has been computed with the settings $m = 15$, $m_S = 6$, and $\mu_{\mathrm{EL}} = 10^{-4}$.

As can be seen in Fig. 5(a) and Fig. 5(b) a feedforward approach is not sufficient, since the system can not follow the desired trajectory. Especially at the end of the motion a feedforward approach leads to large deviations in $q_2(t)$. The resulting errors are $e_{1,\mathrm{FF}}(m) = 5.7°$, $e_{2,\mathrm{FF}}(m) = 38.5°$, and $e_{3,\mathrm{FF}}(m) = 7.1°$ at the finial position. Implementing the controller based on an extended linearization yields much better results with final errors $e_{1,\mathrm{EL}}(m) = 1.9°$, $e_{2,\mathrm{EL}}(m) = -1.1°$, and $e_{3,\mathrm{EL}}(m) = 1.8°$.

B. Nonlinear Online Optimization

In contrast to section VI-A feedforward and feedback input sequences consist of $m = m_S = 6$ values. Furthermore, the constants $\mu_{\mathrm{EL}} = 10^{-6}$ and $\mu_{\mathrm{NO}} = 0.01$ are adopted. The second motion of the manipulator depicted in Fig. 1(a) is from $q_1(0) = 0°$, $q_2(0) = 0°$ to $q_1(mT) = 90°$, $q_2(mT) = 45°$. Choosing initial errors $e_1(0) = 0°$ at the active joint and $e_2(0) = -20°$ at the passive joint leads to the final errors $e_{1,\mathrm{FF}}(m) = 0.1°$, $e_{2,\mathrm{FF}}(m) = 48.9°$ if a feedforward controller is applied, cf. Fig. 6(a). In case the proposed controllers are adopted to counteract the same initial errors as for the feedforward motion in Fig. 6(a) we get the final errors $e_{1,\mathrm{EL}}(m) = 22.9°$, $e_{2,\mathrm{EL}}(m) = 17.1°$ and $e_{1,\mathrm{EL}}(m) = 1.3°$, $e_{2,\mathrm{EL}}(m) = 0.2°$. Both the final errors and the trajectories in Fig. 6(a) point out that the controller based on a nonlinear online optimization is able to reduce large errors much more efficiently than a controller based on an extended linearization.

VII. CONCLUSIONS

Two nonlinear discrete-time controllers for underactuated manipulators operating in the horizontal plane have been proposed. The major benefit of a discrete-time control approach is that the time period in which the system is almost not controllable can be shortened significantly. As has been shown by experimental results, it is even possible to control a highly underactuated manipulator by using a discrete-time control approach based on an extended linearization. To our best knowledge, this is the first time that experimental results of such a manipulator have been presented. In addition, a second control approach based on a nonlinear online

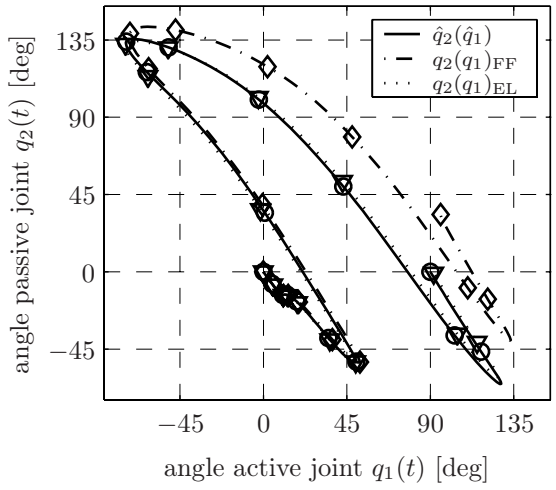

(a) $q_2(t)$ vs. $q_1(t)$

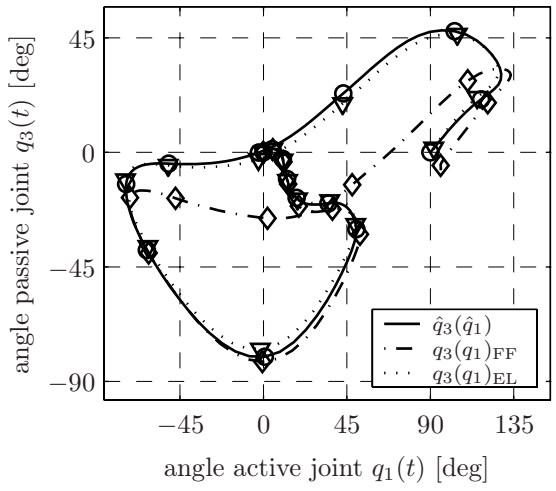

(b) $q_3(t)$ vs. $q_1(t)$

Fig. 5. 90° turn of link 1 (highly underactuated manipulator)

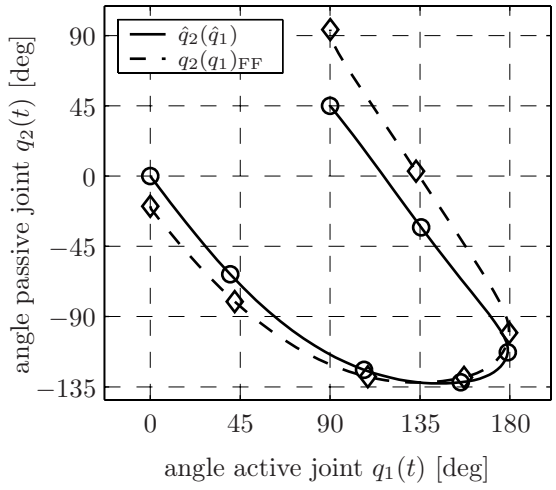

(a) $q_2(t)$ vs. $q_1(t)$ feedforward control

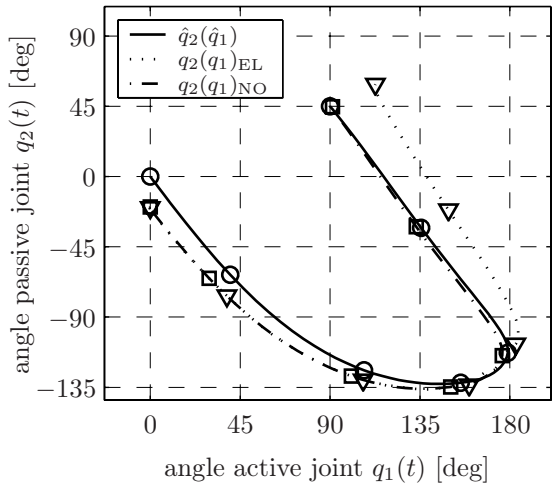

(b) $q_2(t)$ vs. $q_1(t)$ feedback control

Fig. 6. 90° turn of link 1, 45° turn of link 2 (2-DOF underactuated manipulator)

optimization has been proposed concerning the problem that the controller mentioned before is efficient only for small errors. The efficiency of the second controller has been demonstrated by further experimental results of an underactuated manipulator with 2-DOF. Since both controllers do not exploit any structural properties of the manipulators it is likely that they can be used for a large class of underactuated systems.

REFERENCES

[1] H. Arai and S. Tachi, "Position control of a manipulator with passive joints using dynamic couplings," *IEEE Transactions on Robotics and Automation (TRA)*, vol. 7, no. 4, pp. 528–534, 1991.

[2] G. Oriolo and Y. Nakamura, "Control of mechanical systems with second-order nonholonomic constraints: Underactuated manipulators," in *Proc. of the 30th IEEE Conference on Decision and Control (CDC '91)*, Brighton, UK, Dec. 11-13 1991, pp. 2398–2403.

[3] N. Scherm and B. Heimann, "Dynamics and control of underactuated manipulation systems - a discrete-time approach," *Journal of Robotics and Autonomous Systems*, vol. 30, no. 3, pp. 237–248, 2000.

[4] ——, "Discrete-time treatment of underactuated manipulation systems: Dynamics and control," in *Proc. of the 9th International Symposium on Dynamic Problems of Mechanics (DINAME 2001)*, Florianopolis, Brazil, Mar. 5-9 2001, pp. 385–390.

[5] D. Weidemann, N. Scherm, and B. Heimann, "Discrete-time path planning and control of a highly underactuated manipulator," *Machine Intelligence and Robotic Control (MIRoC)*, vol. 4, no. 3, pp. 89–98, 2002.

[6] T. Mita and T. K. Nam, "Control of underactuated manipulators using variable period deadbeat control," in *Proc. of the 18th IEEE International Conference on Robotics and Automation (ICRA 2001)*, Seoul, Korea, May 21-26 2001, pp. 2735–2740.

[7] H. W. Engl, M. Hanke, and A. Neubauer, *Regularization of inverse problems*, ser. Mathematics and its Applications. Dordrecht, Netherlands: Kluwer Academic Publishers, 1996, vol. 375.

[8] J. Nocedal and S. J. Wright, *Numerical optimization*. Berlin, Germany: Springer-Verlag, 1999.

[9] T. Binder, L. Blank, H. G. Bock, R. Bulirsch, W. Dahmen, M. Diehl, T. Kronseder, W. Marquardt, J. P. Schlöder, and O. von Stryk, "Introduction to model based optimization of chemical processes on moving horizons," in *Online Optimization of Large Scale Systems*, S. O. Krumke and J. Rambau, Eds. Berlin, Germany: Springer-Verlag, 2001, pp. 295–339.

[10] M. Diehl, *Real-time optimization for large scale nonlinear processes*, ser. Fortschrittberichte VDI, Meß-, Steuerungs- und Regelungstechnik. Düsseldorf, Germany: VDI Verlag, 2002, vol. 920.

[11] F. Lizarralde, J. T. Wen, and L. Hsu, "A new model predictive control strategy for affine nonlinear control systems," in *Proc. of the American Control Conference (ACC '99)*, San Diego, USA, June 1999, pp. 4263–4267.